Advances in Aeronautical Science and Engineering
ISSN: 1674-8190

Exploring Acetonyl Radical Generation via Photoredox Catalysis in Flow Chemistry.

Luca Moretti[a], Silvia Romano[a], Marco Bianchi,b Alberto Gallo[b]

[a] *Department of Chemistry and Industrial Chemistry, University of Genova, Via Dodecaneso 31, 16100 Genova, Italy.*

[b] *PhotoGreen Lab, Department of Chemistry, University of Pavia, Viale Taramelli 12, 27100 Pavia, Italy.*

ABSTRACT

A Hydrogen Atom Transfer (HAT) step from acetone allowed the smooth generation of acetonyl radical, that was then exploited as synthon in the mild formation of C–C bonds under flow conditions. The process was promoted by aryl radicals photocatalytically generated via Single Electron Transfer (SET) reduction of arenediazonium salts. The mechanism has been investigated by a combined experimental and computational approach and further supported by deuterium labelling experiments.

KEYWORDS

Photocatalysis, Hydrogen Atom Transfer (HAT), Aryl radicals, Arenediazonium salts, Acetonyl radical.

INTRODUCTION

Arenediazonium salts are raising considerable interest as substrates in visible-light photoredox catalyzed processes[1] in view of the smooth preparation and the use as precursors of aryl radicals.[2] A few years ago, König reported the efficient use of arenediazonium salts in photo-Meerwein reactions with styrenes, yielding amides[3] (Scheme 1, path a) or esters[4] (Scheme 1, path b) in a multi-component fashion,[5] depending on the nature of the adopted solvent. The methodology was later extended and applied to the preparation of isochromanones,[6] via the photocatalyzed arylation of styrene derivatives by 2-carboxy substituted arenediazonium salts (Scheme 1, path c). Shortly after, some of us reported that similar results can be smoothly obtained starting from 2-alkoxycarbonyl arenediazonium salts (Scheme 1, path d).[7]

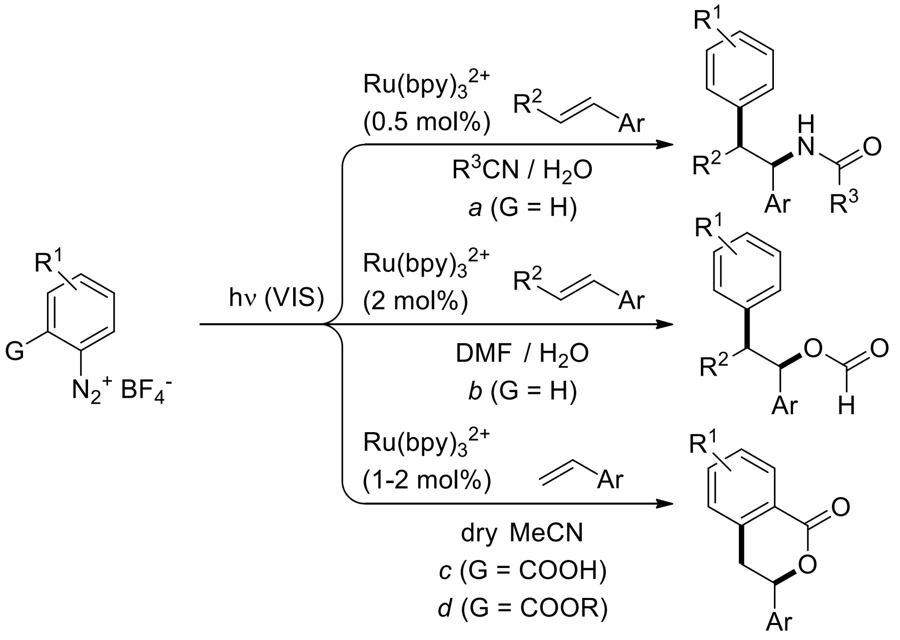

Scheme 1. Photocatalyzed Meerwein reactions for the arylation of styrenes.

RESULTS AND DISCUSSION

Pursuing the studies along this line, we found that the irradiation of arenediazonium salts (e.g. the 4-methoxybenzenediazonium tetrafluoroborate salt **1a**) under analogous conditions in the presence of ethyl 2-vinylbenzoate **2** (Scheme 2, path a) afforded isobenzofuranone **3**.[7] Notably, the reaction was successfully carried out under both batch and continuous flow conditions. In this report, however, we describe a different outcome, since batch irradiation of an equimolar mixture of **1a** and **2** in acetone under dilute conditions (down to 10^{-2} M), in the presence of $[Ru(bpy)_3]Cl_2$ (1 mol%) as the photoredox catalyst, does not lead to the formation of expected **3**, but affords compound **4** instead (Scheme 2, path b), a known natural metabolite of cardiovascular drug *n*-butylphthalide,[8] where a molecule of the solvent has been incorporated in the final product. Notably, we improved the yield of **4** (up to 88% yield) by performing the reaction under continuous flow conditions (flow rate of 10 $mL\cdot h^{-1}$).[9]

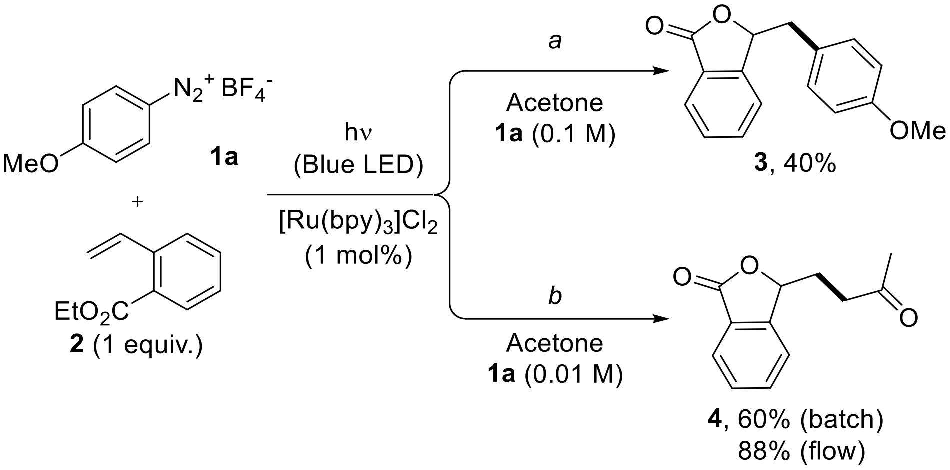

Scheme 2. Concentration-dependent synthesis of isobenzofuranones **3** and **4**.

This result convinced us to investigate more deeply into the nature of the product obtained and, on the basis of the reactivity of aryl radicals,[10] we reasoned that an indirect photocatalytic Hydrogen Atom Transfer (HAT)[11] mechanism could be operative.[12] In our scenario, acetonyl radical $CH_3C(=O)CH_2^{\bullet}$ could be generated from an acetone solvent molecule via hydrogen atom abstraction operated by the aryl radical **Ar**$^{\bullet}$ (Scheme 3, path a) obtained from the photocatalytic reduction of the corresponding arenediazonium salt (path a'). The species $CH_3C(=O)CH_2^{\bullet}$ could then be trapped by the styrene moiety in **2**, to form benzyl radical **5**$^{\bullet}$ (path b). Oxidation of **5**$^{\bullet}$ then afforded benzyl cation **5**$^{+}$ (path c) while restoring the photocatalyst, then ensuing intramolecular cyclization onto the carboxylic group (path d) and elimination of the ethyl group (possibly favored by adventitious water)[13] gave the final product **4**.

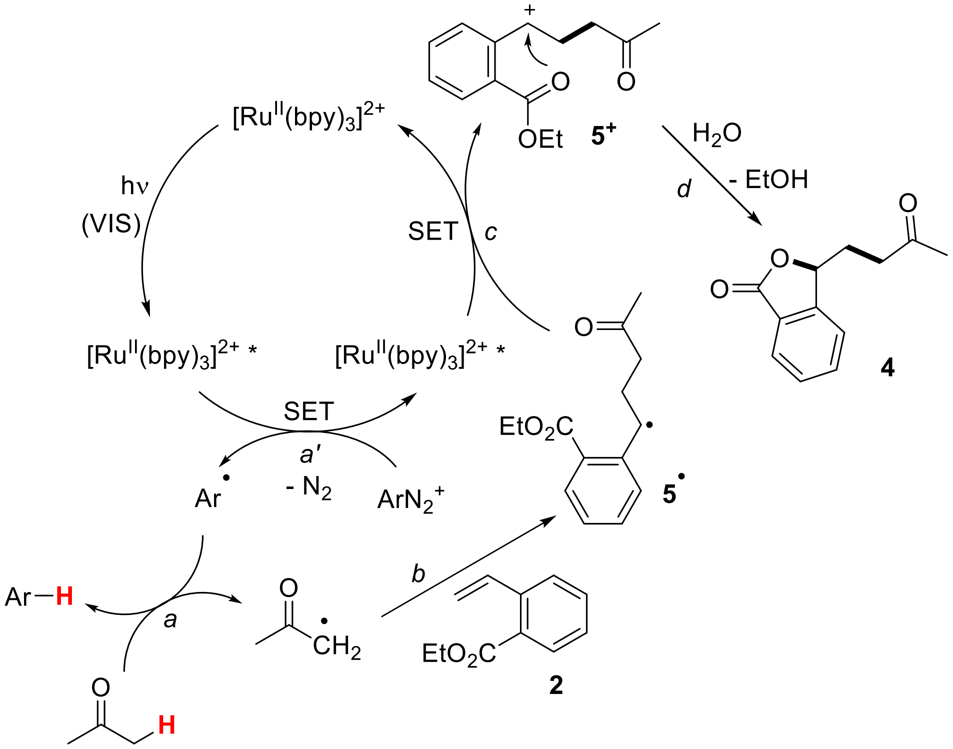

Scheme 3. Proposed mechanism for the formation of **4**.

With the final aim of verifying the suggested mechanism, we supplemented the data available in the literature with a combined theoretical and experimental investigation. The idea was that of analyzing the key steps involved in the proposed mechanism, namely: i) the quenching of the excited state of Ru(bpy)$_3^{2+}$ by arenediazonium salts, ii) the hydrogen atom abstraction from the solvent promoted by the aryl radical and iii) the addition of the photogenerated radicals, either the original aryl radical or that deriving from the solvent, onto methyl 2-vinylbenzoate **2'** (a convenient computational model of **2**).

At first, the reaction was performed, alternatively, in the absence of the diazonium salt or the Ru(II) catalyst, as well as in the dark (irradiation omitted). In all such cases, no traces of product **4** were detected, thus confirming that all the reaction components play a key role in the reaction and that light is mandatory for the desired process to occur. Next, we evaluated the possibility to adopt differently substituted arenediazonium salts in the formation of **4** (Table 1). Noteworthily, we found that the 4-methoxy derivative **1a** was the best in the series, followed by the 4-methyl one (**1b**), yielding **4** in around 90 and 70% isolated yield, respectively, and with a good overall mass balance (see the recovery of **2**). On the other hand, both the 4-fluoro (**1c**) and the 4-chloro (**1d**) derivatives, as well as the parent benzenediazonium salt (**1e**), failed to give **4** in a satisfactory yield (< 50%).

Table 1. Experimental data for the synthesis of **4** promoted by differently substituted arenediazonium salts under optimized flow conditions (see Scheme 2).[a]

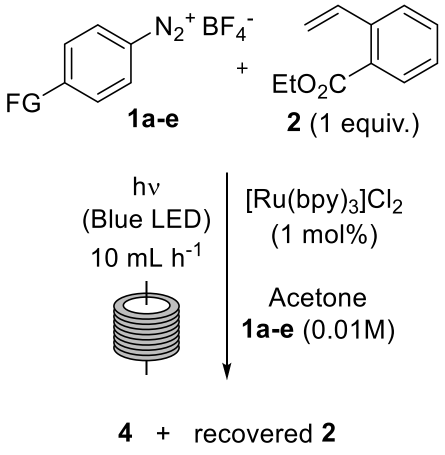

Entry	Diazonium salt, FG =	Yield of 4 (%)	Recovery of 2 (%)
1	**1a** (FG = OMe)	88	7
2	**1b** (FG = Me)	68	18
3	**1c** (FG = F)	5	82
4	**1d** (FG = Cl)	47	51
5	**1e** (FG = H)	39	41

[a] Yields are referred to isolated products after column silica gel chromatography.

Furthermore, we also repeated the reaction between **1a** and **2** in acetonitrile (instead of acetone) under otherwise identical reaction conditions (both batch and flow). Thus, we observed the formation of isobenzofuranone **3**, although in a low yield (23% under flow conditions), while only trace amounts of the compound incorporating the solvent (**6**) were detected by GC-MS analysis (Scheme 4).

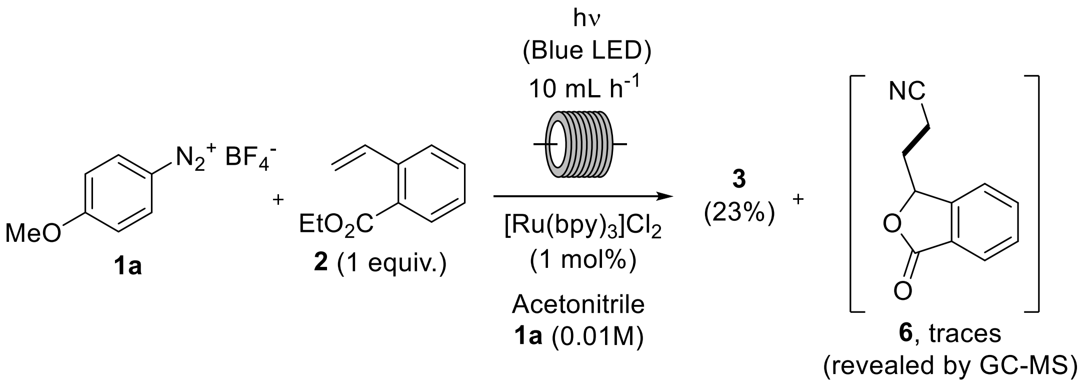

Scheme 4. Attempts to use acetonitrile under the same reaction conditions.

Excited photocatalyst quenching by arenediazonium salts. We initially verified the possibility for the excited $Ru(bpy)_3^{2+}$ photocatalyst to be oxidatively quenched by arenediazonium salts. Thus, the excited state redox potential of the photocatalyst $E(Ru(bpy)_3^{3+}/Ru(bpy)_3^{2+*})$ is largely negative, namely – 0.86 V *vs* SCE.[14] On the other hand, arenediazonium salts are known to be easily reduced and redox potentials $E(ArN_2^+/ArN_2^{\bullet}) < +\ 0.5$ V *vs* SCE have been measured, where the ease of reduction largely depends on the electronic effect of the substituent present on the aromatic ring (e.g. the reduction potential for the 4-nitrobenzenediazonium salt is *ca.* + 0.46-0.50 V *vs* SCE, while that for the 4-methoxybenzenediazonium salt is *ca.* + 0.18-0.19 V *vs* SCE).[15] Accordingly, in all the examined cases the photocatalyst should be competent in triggering the desired mono-electronic reduction step, suggesting that this step cannot be responsible for the differences in reactivity reported in Table 1.

Hydrogen abstraction from the solvent by aryl radicals. Next, we pursued to collect evidences of the HAT step occurring between the proposed aryl radical intermediates and the solvent. Thus, we undertook a theoretical investigation employing the Density Functional Theory (DFT) approach. In particular, the relevant geometries have been optimized adopting the (unrestricted) ωB97XD functional with the 6-31G(d,p) basis set in the gas phase. Careful inspection of the frequency calculations performed on the optimized geometries at the same level of theory allowed to identify the stationary points either as minima or transition states. In the latter case, it was verified as well that the only imaginary frequency described the motion along the desired reaction coordinate. Finally, solvent effects were included via single point calculations adopting the implicit SMD model and either acetone or acetonitrile as the reaction medium (see Section S4 in the Supporting Information for further details).

Table 2. Computational data for relevant H-abstraction processes promoted by differently substituted aryl radicals.[a]

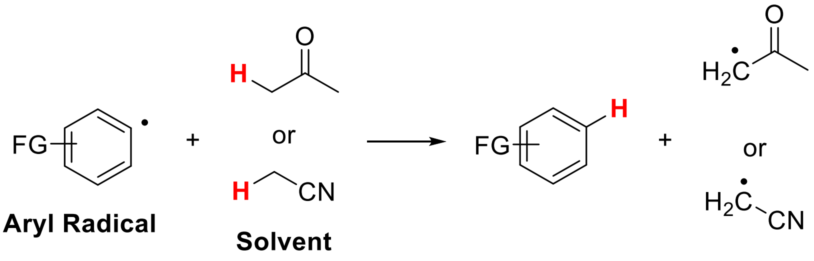

Entry	Aryl Radical FG =	Solvent	$\Delta G^{\ddagger}$ [kcal·mol^{-1}]	ΔG [kcal·mol^{-1}]
1	4-OMe	Acetone	10.49	-16.68

2	4-Me	Acetone	10.55	-15.93
3	4-F	Acetone	10.94	-16.83
4	4-Cl	Acetone	10.95	-16.69
5	H	Acetone	11.24	-15.63
6	2-COOMe	Acetone	10.69	-16.64
7	4-OMe	Acetonitrile	10.68	-16.66

[a] Energy values expressed in kcal·mol^{-1} at the SMD-ωB97XD/6-31G(d,p) level of theory in bulk acetone or acetonitrile (see the “Solvent” column) have been reported (see Table S1 in the SI for details).

As reported in Table 2, the efficiency of (substituted) aryl radicals in promoting the HAT step from acetone depends on the nature of the aromatic substituent, if any. Whereas all the examined processes occur with a largely negative Gibbs free energy change (ΔG), different trends can be identified in terms of Gibbs free energy barriers ($\Delta G^{\ddagger}$). Thus, while the 4-methyl and the 4-methoxy substituted aryl radicals show $\Delta G^{\ddagger}$ values around + 10.5 kcal·mol^{-1} (entries 1, 2), the 4-halogen substituted and the unsubstituted derivatives (entries 3-6) show higher barriers, around + 11.0 kcal·mol^{-1}, with the species bearing a 2-methoxycarbonyl group ranking in between (*ca.* + 10.7 kcal·mol^{-1}). As indicated in Table 2, entry 7, we also verified computationally the possibility to cleave the C–H bond in acetonitrile by taking the *p*-methoxy aryl radical as model H-abstracting species. The latter process was predicted to occur with a $\Delta G^{\ddagger}$ value around + 10.7 kcal·mol^{-1}, a slightly higher barrier if compared with that of acetone ($\Delta\Delta G^{\ddagger}$ *ca.* + 0.20 kcal·mol^{-1}).

Interestingly, the reaction profile of the model reaction describing the hydrogen atom abstraction from acetone promoted by the 4-methoxyphenyl radical is reported in Figure 1, along with the structure of the involved transition state (TS). Indeed, it is apparent that the reaction occurs with an early TS, as highlighted by the shorter $CH_3C(=O)CH_2\cdots H$ distance (1.24 Å, blue color in Figure 1) than the $Ar\cdots H$ distance (1.46 Å, orange color), a typical case of largely exergonic processes. Accordingly, even if small differences in $\Delta G^{\ddagger}$ values ($\Delta\Delta G^{\ddagger} < 1$ kcal·mol^{-1}) have been observed when considering the H-abstraction operated by different aryl radicals, these values can still be considered as indicative of a different reactivity and the small gaps can be related to the intrinsic character of the modeled processes. As a matter of fact, there is a close agreement between the experimental data gathered in Table 1 and the computational ones in Table 2, showcasing the importance of this H-abstraction step for the occurrence of the investigated reaction.

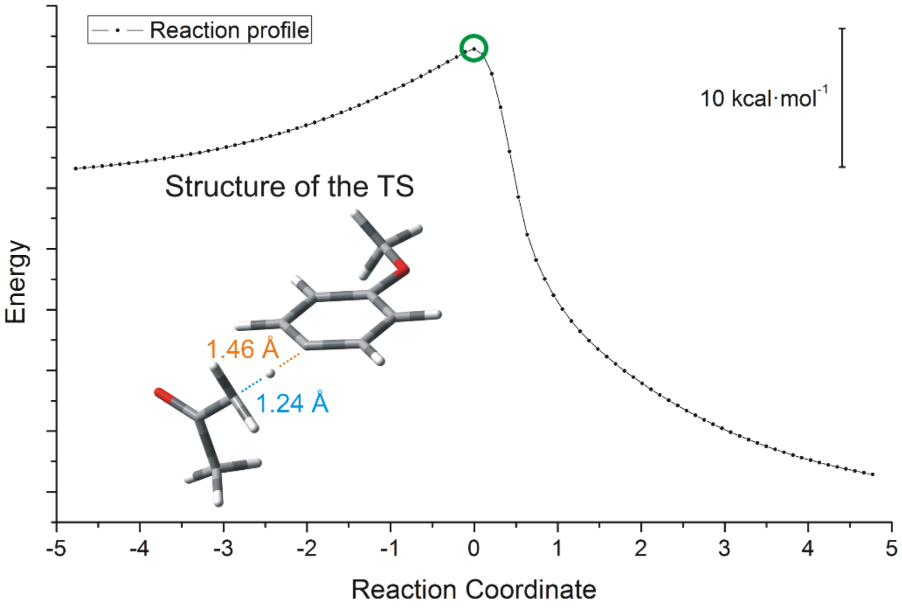

Figure 1. Reaction profile of the hydrogen atom abstraction process from acetone by the 4-methoxyphenyl radical, along with the structure of the transition state (TS, highlighted in the green circle) and a few relevant geometric parameters.

Deuterium labelling experiments. To further confirm the role of the HAT step promoted by the aryl radical, the reaction was carried out by using the 2-(4-methoxybenzyloxy)carbonyl benzenediazonium salt **1f**, since the 4-methoxybenzyloxycarbonyl substituent facilitated TLC detection and chromatographic purification of the corresponding reduced derivative, while remaining inert during the reaction. Furthermore, according to the computational data reported above, the presence of a -COOMe group *ortho*- to the aryl radical site should not hamper the HAT reactivity of this intermediate (see Table 2, entry 6). Accordingly, irradiation of **1f** in acetone under the conditions described above gave equimolar amounts of 4-methoxybenzyl benzoate **7** (73%) and product **4** (73%; Scheme 5, upper part). On top of that, when the reaction was carried out in hexadeuteroacetone, the process required a longer irradiation time (5 mL·h^{-1} flow rate adopted) and yielded 4-methoxybenzyl 2-deuterobenzoate **7-*d*$_1$** and pentadeuterated product **4-*d*$_5$**, again in comparable yields (83 and 90%, respectively; Scheme 5, lower part). Taken together, these experiments confirm the need to use a stoichiometric amount of the starting arenediazonium salt for the desired process to take place, further corroborating the proposed mechanism. The kinetic isotope effect (KIE) of the reaction was measured as well by running the same experiment in a 1:1 mixture of acetone and hexadeuteroacetone with a flow rate of 5 mL·h^{-1}: the ratio of **7** and **7-*d*$_1$** was found to be 6.5:1, as determined by GC-MS analysis (a similar ratio of **4** and **4-*d*$_5$** was found, *viz.* 7:1), pointing out a primary kinetic isotope effect for the investigated process.

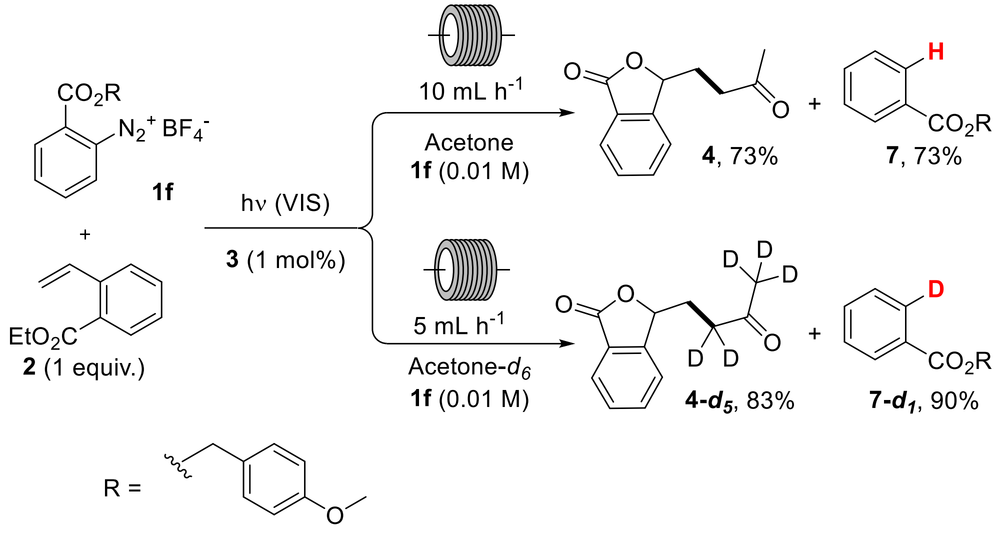

Scheme 5. Experiments carried out to demonstrate the role of arenediazonium salts in the reaction mechanism.

Addition of the photogenerated radicals onto 2-vinylbenzoate ester. As hinted above, we also modeled the addition of the photogenerated radicals onto the olefinic reaction partner present in solution, *viz.* methyl 2-vinylbenzoate **2'**, taken as a computational model of **2** (Table 3). Also, in this case, the investigated processes can be grouped according to two different categories. The first one describes the addition of the *p*-methoxyphenyl radical onto **2'**, a process that occurs with a very small Gibbs free energy barrier ($\Delta G^{\ddagger}$ *ca.* + 6.00 $kcal{\cdot}mol^{-1}$), independently from the adopted solvent (acetone or acetonitrile; see entries 1, 2). At the same time, the process is accompanied by a largely negative Gibbs free energy change, around – 40 $kcal{\cdot}mol^{-1}$. By contrast, the addition of the acetonyl radical $CH_3C(=O)CH_2^{\bullet}$ or the cyanomethyl radical $NCCH_2^{\bullet}$ occurs with less favorable parameters (entries 3, 4), as highlighted by the more positive $\Delta G^{\ddagger}$ (*ca.* + 10.9 and + 11.5 $kcal{\cdot}mol^{-1}$, respectively) and less negative ΔG values (*ca.* – 20.2 and – 19.1 $kcal{\cdot}mol^{-1}$, respectively). Indeed, these data confirm the lower tendency of the cyanomethyl radical towards the addition onto **2** compared to the acetonyl radical, with a $\Delta\Delta G^{\ddagger}$ value around + 0.60 $kcal{\cdot}mol^{-1}$.

Table 3. Computational data for relevant radical addition processes onto methyl 2-vinylbenzoate **2'**.[a]

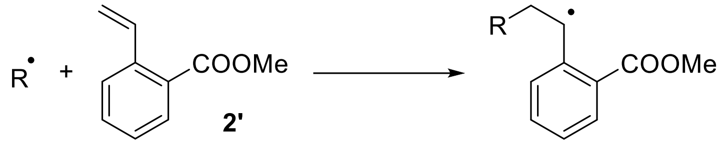

Entry	Radical R• =	Solvent	ΔG‡ [kcal·mol⁻¹]	ΔG [kcal·mol⁻¹]
1	4-MeO$C_6H_4^•$	Acetone	6.02	-39.27
2	4-MeO$C_6H_4^•$	Acetonitrile	5.96	-39.21
3	$CH_3COCH_2^•$	Acetone	10.89	-20.24
4	$NCCH_2^•$	Acetonitrile	11.52	-19.14

[a] Energy values expressed in kcal·mol^{-1} at the SMD-ωB97XD/6-31G(d,p) level of theory in bulk acetone or acetonitrile (see the “Solvent” column) have been reported (see Table S2 in the SI for details).

Taken together, the computational evidences well match with the experimental outcome reported in Table 1. First, the simulations clearly highlight the fundamental role of generating a good H-abstracting species (4-MeO$C_6H_4^•$) for the desired process to take place satisfactorily. When the 4-F, 4-Cl or 4-H aryl radicals are involved, on the other hand, the occurrence of undesired side processes partially inhibits the reaction, probably due to a poor turnover of the catalytic system.

Furthermore, the experimental results obtained when running the reaction in acetonitrile (see Scheme 4) can be ascribed to two main reasons, namely: i) HAT step from acetonitrile is not occurring or ii) the cyanomethyl radical is indeed generated, but does not add to the double bond, again inhibiting the turnover of the catalytic system and leading to poor results. Thus, the computational analysis seems to point towards the second hypothesis, since a marked difference between the behavior of acetone *vs* acetonitrile has been observed only in the second step (with a $\Delta\Delta G^‡$ value around + 0.60 kcal·mol^{-1}). Furthermore, this is also in accordance with previous reports in the literature, that highlighted the possibility to generate and trap both acetonyl and cyanomethyl radicals with a methacrylamide reaction partner under similar reaction conditions.[16] Accordingly, we do believe that the 4-methoxyphenyl radical is indeed capable to cleave the C–H bond both in acetone and acetonitrile, but in the latter case the radical trap employed here is not suitable for intercepting the cyanomethyl radical, triggering the occurrence of parasite pathways that shut down the catalytic cycle.

Overall, provided that the optimal reaction partners are chosen, the computational work corroborates the fundamental role of the concentration parameter. Thus, the high reactivity of aryl radicals towards olefins can be prevented only under highly diluted conditions, in order to minimize the chance for the aryl radical to interact and add onto the π-bond trap, in turn shifting the reactivity towards the desired HAT from the solvent.

Intrigued therefore by the novelty of our findings and specifically by the mildness of the conditions employed to generate the acetonyl radical, we extended this strategy to other substrates able to undergo a similar radical cyclization. Accordingly, we tested the reactivity of ethyl propenylbenzoate **8** (displaying a more challenging internal double bond), *N*-methyl-*N*-phenyl methacrylamide **10** (recently employed as trap of acetonyl and cyanomethyl radicals)[16,17] and phenylpropiolate **12** under optimized reaction conditions. Indeed, the desired products, including isobenzofuranone **9**, oxindole **11** and coumarin **13** (already prepared through a similar cascade process using excess peroxides at high temperature),[18] were obtained in decent yields (Scheme 6). Thus, **9** was isolated in 25% yield (55% based on the consumption of **8**) in a process involving a rather unusual (for this kind of reactions) β-substituted styrene as the starting substrate. On the other hand, irradiation of **1a** in acetone in the presence of **10** afforded the desired oxindole **11** in 50% yield (93% based on the consumption of the starting substrate), whereas ketocoumarin **13** was isolated in discrete yield via an acetonyl radical induced cyclization of **12**.

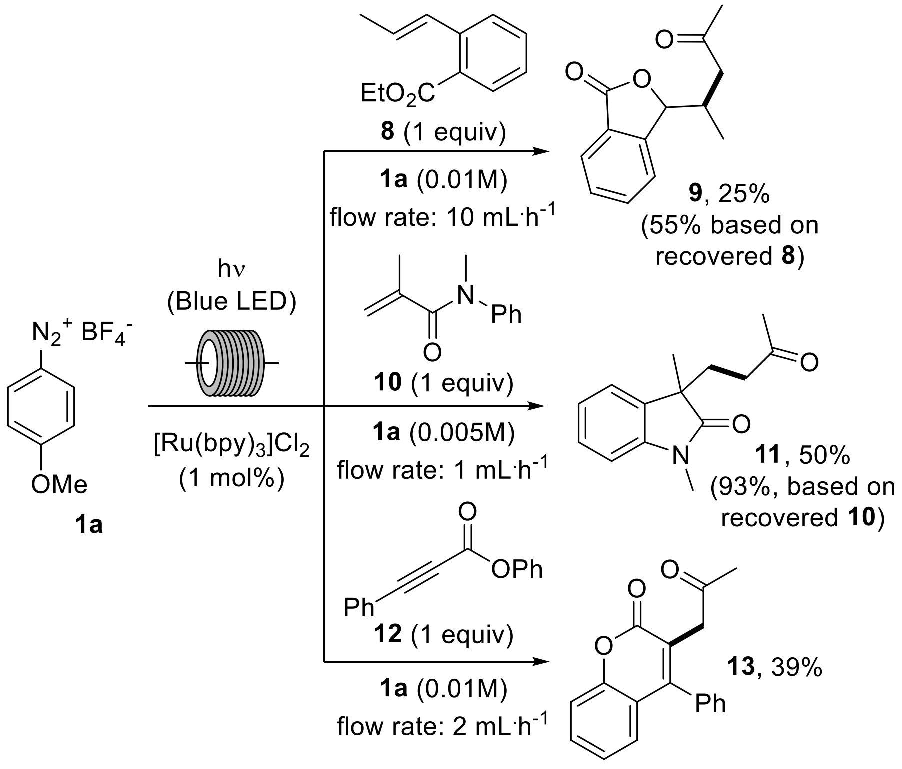

Scheme 6. Acetonyl radical induced synthesis of heterocycles **9**, **11** and **13**.

However, the electrophilic nature[19] of the acetonyl radical suggested that reaction with electron-rich olefins, such as silyl enol ethers, could be a favorable process, in turn able to afford valuable 1,4-dicarbonyl derivatives. The photocatalytic addition of acetonyl radical to enol ether derivatives under flow conditions could represent a mild and valuable alternative to existing procedures to assemble such compounds.[20]

To this aim, we reacted arenediazonium salt **1a** with silyl enol ether **14a** (derived from acetophenone) in acetone, under the optimized continuous flow conditions described above, using a flow rate of 10 mL·h^{-1}. The desired product **15a** was isolated in 91% yield. The same reaction under batch conditions afforded only 17% of the desired product after 24 hrs. On the other hand, when acetophenone was used in place of **14a**, no acetonyl radical addition occurred, as expected.

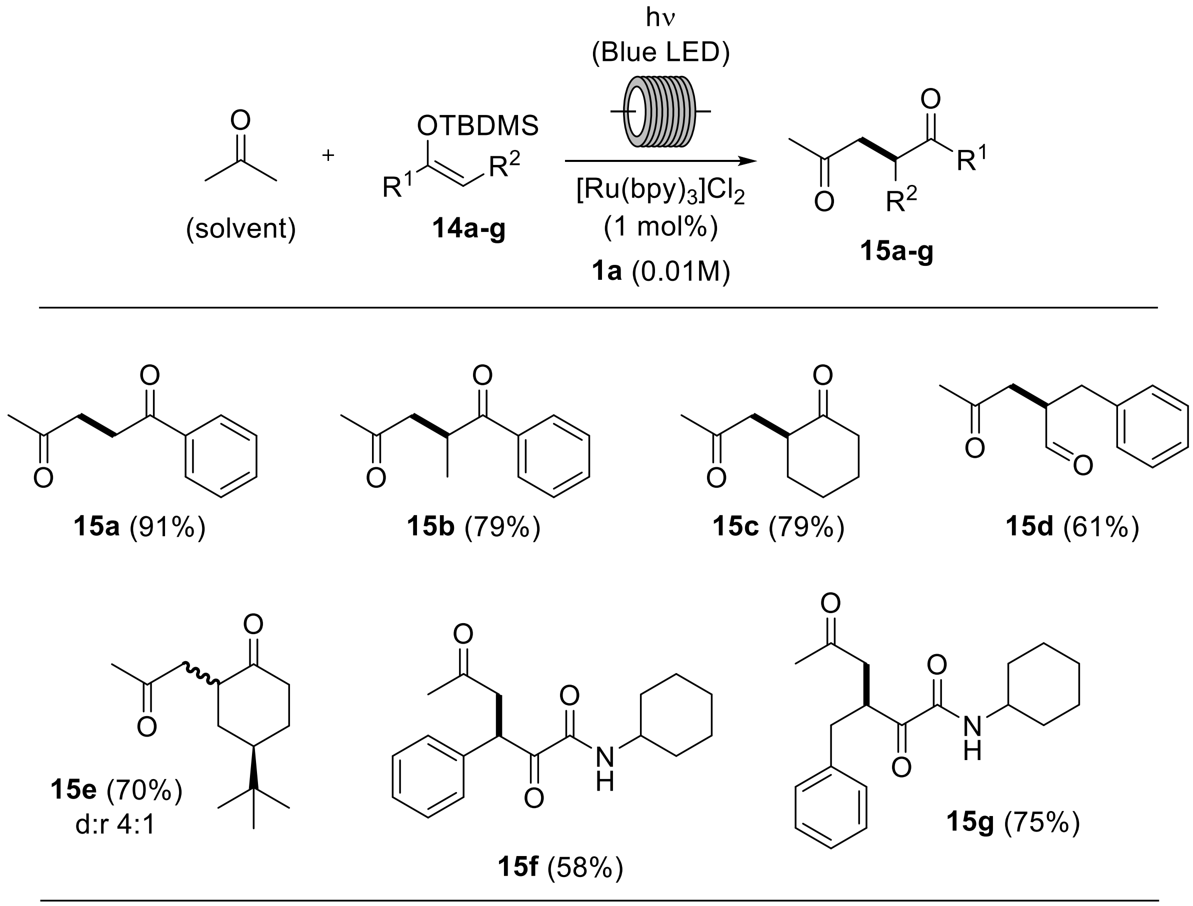

Scheme 7. Photocatalytic synthesis of 1,4-diketones via acetonyl radical.

The versatility of the proposed methodology was further demonstrated by extending the protocol to other silyl enol ethers (**14b-g**), and the results are reported in Scheme 7. Noteworthy, products **15f-g** were synthesized from silyl enol ethers prepared according to a photoinduced silylative-ketene-three-component-reaction recently disclosed by some of us.[21] Accordingly, the synthesis of compound **15g** was also optimized in a one-pot fashion. Thus, diazoketone **16**, silanol **17** and isocyanide **18** were irradiated in toluene (0.5 M) to induce the formation of the silyl enol ether **14g**. Upon consumption of the diazoketone, the solution was diluted with acetone (up to 0.01 M, based on a theoretical 100% yield for **14g**), then diazonium salt **1a** and the photocatalyst $[Ru(bpy)_3]^{2+}$ were added and the resulting mixture flown through the flow apparatus at a 3 $mL \cdot h^{-1}$ flow rate. Compound **15g** was successfully isolated, after chromatographic purification, in 40% overall yield, thus demonstrating that the present acetonylation methodology is also compatible with crude mixtures deriving from a multi-component process (Scheme 8). Finally, since 1,4-dicarbonyls are extensively used in organic synthesis, for example in the Paal-Knorr reaction towards five-membered heteroarenes,[22] compound **15g** was reacted with benzylamine in the presence of acetic acid, giving highly functionalized pyrrole **19** in 59% yield (Scheme 8).

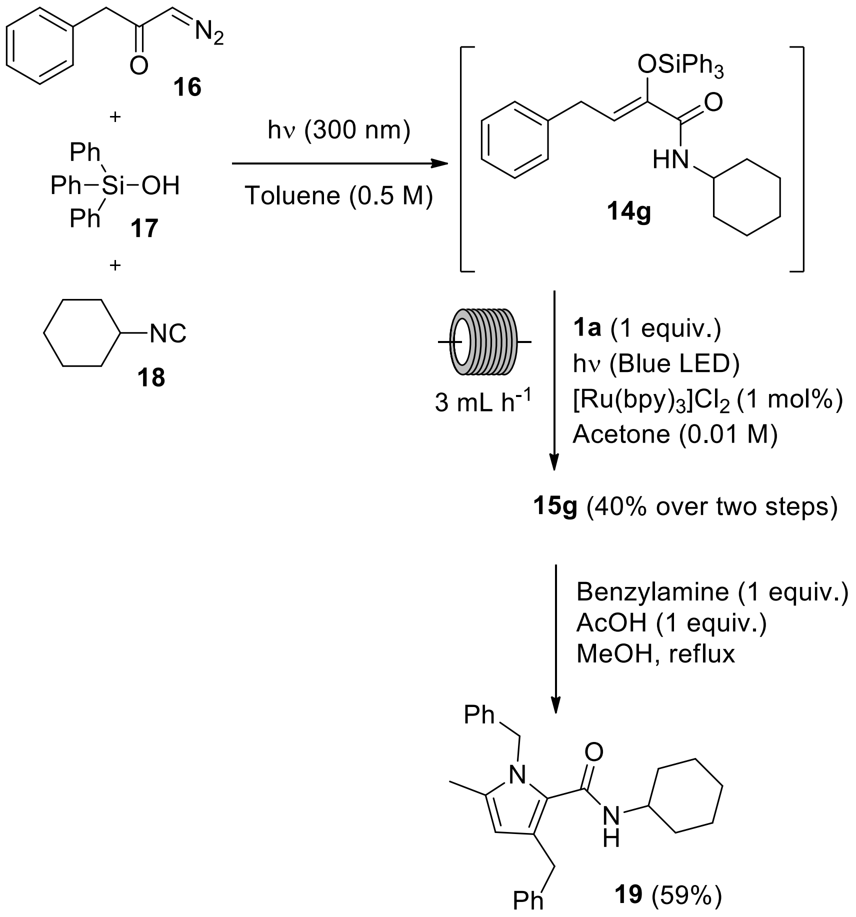

Scheme 8. One-pot synthesis of 1,4-dicarbonyl **15g** via silylative-ketene-three-component-reaction and acetonylation of the resulting silyl enol ether, followed by Paal-Knorr process to give pyrrole **19**.

Acetonyl radical has recently attracted the scientific community for his surprisingly high concentration in the troposphere and its role in affecting NO_X, HO_X and O_3 cycling.[23] However, its application in synthesis is rather limited and not exempt from drawbacks. For example, its generation is usually accomplished by employing an excess of an oxidant (hydroperoxides, MnO_2) and high temperatures as well as prolonged reaction times are commonly required.[16-18,24] On the other hand, the reaction conditions presented here require only 1 mol% of a photoredox catalyst, together with a stoichiometric amount of a diazonium salt as the aryl radical precursor. The generation of the acetonyl radical proceeds at room temperature in diluted solutions, and application of a flow system, whose advantages in photocatalysis are well recognized,[25] allows also for overcoming the safety issues related to the use of diazonium salts. Furthermore, our conditions have been proven compatible with a wide variety of (relatively unstable) silyl enol ethers.

CONCLUSIONS

In conclusion, we have reported that acetonyl radical can be generated from the combination of arenediazonium salts and the well-known $[Ru(bpy)_3]^{2+}$ photocatalyst dissolved in acetone under blue LED irradiation. The reaction proceeds via the formation of an aryl radical and subsequent HAT from the solvent. Diluted conditions have shown to prevent the typical addition of aryl radicals to C=C bonds and the application of a flow system has been beneficial for the reaction, overcoming safety issues usually associated with the handling of diazonium salts and improving reaction yields compared to the batch processes. The optimized methodology has been exploited to highlight the synthetic relevance of this investigation, since acetonyl radical can be efficiently used as synthon to prepare 1,4-dicarbonyl derivatives through a formal *umpolung* reactivity mode.

ASSOCIATED CONTENT

General experimental methods, details on experimental procedures, analytical data, computational analyses and copies of ^{1}H and ^{13}C NMR spectra. This material is available free of charge via the Internet at http://pubs.acs.org.

ACKNOWLEDGEMENTS

D.R. thanks the MIUR for financial support (SIR Project “Organic Synthesis via Visible Light Photocatalytic Hydrogen Transfer”; Code: RBSI145Y9R). Calculations were carried out at the CINECA Supercomputer Center (Italy), with computer time granted by ISCRA projects (code: HP10CSWOH1).

References

(1) For a review, see: (a) Mo, F.; Dong, G.; Zhang, Y.; Wang, J. Recent Applications of Arene Diazonium Salts in Organic Synthesis. *Org. Biomol. Chem*. **2013**, *11*, 1582-1593; for recent examples, see: (b) Majek M.; von Wangelin A. J. Metal-free Carbonylations by Photoredox Catalysis. *Angew. Chem. Int. Ed.* **2015** *54*, 2270-2274; (c) Akram, M. O.; Mali, P. S.; Patil, N. T. Cross-Coupling Reactions of Aryldiazonium Salts with Allylsilanes under Merged Gold/Visible-Light Photoredox Catalysis. *Org. Lett*. **2017**, *19*, 3075-3078; (d) Tlahuext-Aca, A.; Hopkinson, M. N.; Daniliuc, C. G.; Glorius, F. Oxidative Addition to Gold(I) by Photoredox Catalysis: Straightforward Access to Diverse (C,N)-Cyclometalated Gold(III) Complexes. *Chem. Eur. J.* **2016**, *22*, 11587-11592; (e) Xia, Z.; Khaled, O.; Mouriès-Mansuy, V.; Ollivier, C.; Fensterbank, C. Dual Photoredox/Gold Catalysis Arylative Cyclization of *o*-Alkynylphenols with Aryldiazonium Salts: A Flexible Synthesis of Benzofurans. *J. Org. Chem.* **2016**, *81*, 7182-7190; (f) Tlahuext-Aca, T.; Hopkinson, M. N.; Sahoo, B.; Glorius, F. Dual Gold/Photoredox-Catalyzed C(sp)–H Arylation of Terminal Alkynes with Diazonium Salts. *Chem Sci*. **2016**, *7*, 89-93; (g) Bottecchia, C; Rubens, M.; Gunoo, S. B.; Hessel, V.; Madder, A.; Noël, T. Visible-Light-Mediated Selective Arylation of Cysteine in Batch and Flow. *Angew. Chem. Int. Ed.* **2017**, *56*, 12701-12707.

(2) Ghosh, I.; Marzo, L.; Das, A.; Shaikh, R.; König, B. Visible Light Mediated Photoredox Catalytic Arylation Reactions. *Acc. Chem. Res.* **2016**, *49*, 1566-1577.

(3) (a) Hari, D. P.; König, B. The Photocatalyzed Meerwein Arylation: Classic Reaction of Aryl Diazonium Salts in a New Light. *Angew. Chem. Int. Ed.* **2013**, *52*, 4734-4743; (b) Hari, D. P.; Hering, T.; König, B. The Photoredox-Catalyzed Meerwein Addition Reaction: Intermolecular Amino-Arylation of Alkenes. *Angew. Chem. Int. Ed*. **2014**, *53*, 725-728.

(4) Yao, C.-J.; Sun, Q.; Rastogi, N.; König, B. Intermolecular Formyloxyarylation of Alkenes by Photoredox Meerwein Reaction. *ACS Catal*. **2015**, *5*, 2935-2938.

(5) For a review on photocatalyzed multicomponent reactions, see: Garbarino S.; Ravelli, D.; Protti, S.; Basso, A. Photoinduced Multicomponent Reactions. *Angew. Chem. Int. Ed.* **2016**, *55*, 15476-15484.

(6) Crespi, S.; Jäger, S.; König, B.; Fagnoni, M. A Photocatalytic Meerwein Approach to the Synthesis of Isochromanones and Isochromenones. *Eur. J. Org. Chem.* **2017**, *2017*, 2147-2153.

(7) Anselmo, M.; Moni, L.; Ismail, H.; Comoretto, S.; Riva, R.; Basso, A. Photocatalyzed Synthesis of Isochromanones and Isobenzofuranones under Batch and Flow Conditions. *Beilstein J. Org. Chem.* **2017**, *13*, 1456-1462.

(8) Diao, X.; Deng, P.; Xie, C.; Li, X.; Zhong, D.; Zhang Y.; Chen, X. Metabolism and Pharmacokinetics of 3-*n*-Butylphthalide (NBP) in Humans: The Role of Cytochrome P450s and Alcohol Dehydrogenase in Biotransformation. *Drug Metab. Dispos.* **2013**, *41*, 430-444.

(9) The in-house made flow apparatus has already been described in Ref. 7.

(10) For a review, see: (a) Galli, C. Radical Reactions of Arenediazonium Ions: An Easy Entry into the Chemistry of the Aryl Radical. *Chem. Rev.* **1988**, *88*, 765-792; for a recent example, see: (b) Majek, M.; Filace, F.; Jacobi von Wangelin, A. Visible Light Driven Hydro-/Deuterodefunctionalization of Anilines. *Chem. Eur. J.* **2015**, *21*, 4518-4522.

(11) Special issue on “Hydrogen Atom Transfer”, see: Costas, M.; Bietti, M. Uncovering the Complexity of the Simplest Atom Transfer Reaction. *Acc. Chem. Res.* **2018**, *51*, 2601-2602.

(12) (a) Capaldo, L.; Ravelli, D. Hydrogen Atom Transfer (HAT): A Versatile Strategy for Substrate Activation in Photocatalyzed Organic Synthesis. *Eur. J. Org. Chem.* **2017**, *2017*, 2056-2071; (b) Protti, S.; Fagnoni, M.; Ravelli, D. Photocatalytic C–H Activation by Hydrogen-Atom Transfer in Synthesis. *ChemCatChem* **2015**, *7*, 1516-1523.

(13) The elimination of the alkyl group during the cyclization step was already discussed in Ref. 7.

(14) Narayanam, J. M. R.; Stephenson, C. R. J. Visible Light Photoredox Catalysis: Applications in Organic Synthesis. *Chem. Soc. Rev.* **2011**, *40*, 102-113.

(15) (a) Koval'chuk, E. P.; Obushak, N. D.; Ganushchak, N. I.; Yanderka, P. Polarographic Investigation of the Reduction of para-Substituted Arenediazonium Salts. *J. Gen. Chem. USSR (Engl. Transl.)* **1986**, *56*, 1671-1674; (b) Fanghänel, E.; Kriwanek, J.; Ortmann, W.; Bagal, I. L.; Lebedeva, N. W.; El'cov, A. V. Elektrochemische Reduktion und Azokupplung Kernchlorierter *p*-Dimethylaminobenzendiazoniumsalze Hammett-Korrelationen. *J. Prakt. Chem.* **1985**, *327*, 80-84.

(16) Zhang, J.-L.; Liu, Y.; Song, R.-J.; Jiang, G.-F.; Li, J.-H. 1,2-Alkylarylation of Activated Alkenes with Two C–H Bonds by Using Visible-Light Catalysis. *Synlett* **2014**, *25*, 1031-1035.

(17) (a) Xia, X.-F.; Zhu, S.-L.; Zeng, M.; Gu, Z.; Wang, H.; Li, W. Acid-Catalyzed Cascade Radical Addition/Cyclization of Arylacrylamides with Ketones. *Tetrahedron* **2015**, *71*, 6099-6103; (b) Boess, E.; Karanestora, S.; Bosnidou, A.-E.; Schweitzer-Chaput, B.; Hasenbeck, M.; Klussmann, M. Synthesis of Oxindoles by Brønsted Acid Catalyzed Radical Cascade Addition of Ketones. *Synlett* **2015**, 1973-1976.

(18) (a) Pan, C.; Chen, R.; Shao, W.; Yu, J.-T. Metal-Free Radical Addition/Cyclization of Alkynoates with Xanthates towards 3-(β-Carbonyl)coumarins. *Org. Biomol. Chem.* **2016**, *14*, 9033-9039; (b) Yu, Y.; Zhuang, S.; Liu, P.; Sun, P. Cyanomethylation and Cyclization of Aryl

Alkynoates with Acetonitrile under Transition-Metal-Free Conditions: Synthesis of 3-Cyanomethylated Coumarins. *J. Org. Chem*., **2016**, *81*, 11489-11495.

(19) (a) Min, R. S.; Aksenov, V. S.; Vinogradov, M. G.; Nikishin, G. I. Radical Reaction of Acetone with Aromatic Compounds. *Bull. Acad. Sci. USSR, Div. Chem. Sci.* **1979**, *28*, 2114-2117; (b) Gardrat, C. Acetonylation Aromatique Homolitique. *Bull. Soc. Chim. Belg.* **1984**, *93*, 897-901.

(20) See for instance: (a) Noyori, R.; Nishida, I.; Sakata, J. Tris(dialkylamino)sulfonium Enolates. Synthesis, Structure, and Reactions. *J. Am. Chem. Soc.* **1983**, *105*, 1598-1608; (b) Luo, J.; Jiang, Q.; Chen, H.; Tang, Q. Catalyst-Free Formation of 1,4-Diketones by Addition of Silyl Enolates to Oxyallyl Zwitterions in Situ Generated from α-Haloketones. *RSC Adv.* **2015**, *5*, 67901-67908; (c) Arceo, E.; Montroni, E.; Melchiorre, P. Photo-Organocatalysis of Atom-Transfer Radical Additions to Alkenes. *Angew. Chem., Int. Ed.* **2014**, *53*, 12064-12068; (d) Usugi, S.; Yorimitsu, H.; Shinokubo, H.; Oshima, K. Triethylborane Induced Radical Reaction of Gallium Enolates with α -Halo Esters. *Bull. Chem. Soc. Jpn.* **2002**, *75*, 2049-2052; for a recent example exploiting a visible light mediated approach, see: (e) Esumi, N.; Suzuki, K.; Nishimoto, Y.; Yasuda, M. Synthesis of 1,4-Dicarbonyl Compounds from Silyl Enol Ethers and Bromocarbonyls, Catalyzed by an Organic Dye under Visible-Light Irradiation with Perfect Selectivity for the Halide Moiety over the Carbonyl Group. *Org. Lett.* **2016**, *18*, 5704-5707; for a recent example of the use of silyl enol ethers as radical traps, see: (f) Pettersson, F.; Bergonzini, G.; Cassani, C.; Wallentin, C.-J. Redox-Neutral Dual Functionalization of Electron-Deficient Alkenes. *Chem. Eur. J.* **2017**, *23*, 7444-7447.

(21) Ibba, F.; Capurro, P.; Garbarino, S.; Anselmo, M.; Moni, L.; Basso, A. Photoinduced Multicomponent Synthesis of α-Silyloxy Acrylamides, an Unexplored Class of Silyl Enol Ethers. *Org. Lett.* **2018**, *20*, 1098-1101.

(22) Khaghaninejad, S.; Heravi, M. M.; In *Advances in Heterocyclic Chemis*try; Katritzky, A. R. Ed.; Elsevier Academic Press: San Diego, USA, 2014, Vol. 111, pp. 95-146.

(23) (a) Espinosa-García, J.; Márquez, A.; Dóbé, S. Theoretical Enthalpy of Formation of the Acetonyl Radical. *Chem. Phys. Lett.* **2003**, *373*, 350-356; (b) El-Nahas, A. M.; Bozzelli, J. W.; Simmie, J. M.; Navarro, M. V.; Black, G.; Curran, H. J. Thermochemistry of Acetonyl and Related Radicals. *J. Phys. Chem. A* **2006**, *110*, 13618-13623; (c) Imrik, K.; Farkas, E.; Vasvári, G.; Szilágyi, I.; Sarzyński, D.; Dóbé, S.; Bérces, T.; Márta, F. Laser Spectrometry and Kinetics of Selected Elementary Reactions of the Acetonyl Radical. *Phys. Chem. Chem. Phys.* **2004**, *6*, 3958-3968; (d) Zügner, G. L.; Szabó, E.; Farkas, M.; Dóbé, S.; Brudnik, K.; Sarzyński, D.; Jodkowski, J. T. Kinetics and Mechanism of the Reaction of Acetonyl Radical, $CH_3C(O)CH_2$, with Br_2. *Chem. Phys. Lett.* **2013**, *568-569*, 59-62.

(24) (a) Shiraishi, Y.; Tsukamoto, D.; Hirai, T. Highly Efficient Methyl Ketone Synthesis by Water-Assisted C−C Coupling between Olefins and Photoactivated Acetone. *Org. Lett.* **2008**, *10*, 3117-3120; (b) Zhu, L.; Chen, H.; Wang, Z.; Li, C. Formal Fluorine Atom Transfer Radical Addition: Silver-Catalyzed Carbofluorination of Unactivated Alkenes with Ketones in Aqueous Solution. *Org. Chem. Front.* **2014**, *1*, 1299-1305; (c) Schweitzer-Chaput, B.; Demaerel, J.; Engler, H.; Klussmann M. Acid-Catalyzed Oxidative Radical Addition of Ketones to Olefins. *Angew. Chem., Int. Ed.* **2014**, *53*, 8737-8740; (d) Chu, X.-Q.; Meng, H.; Zi, Y.; Xu, X.-P.; Ji S.-J. Metal-Free Oxidative Radical Addition of Carbonyl Compounds to α,α-Diaryl Allylic Alcohols: Synthesis of Highly Functionalized Ketones. *Chem. Eur. J.* **2014**, *20*, 17198-17206; (e) Lan, X.-W.; Wang, N.-X.; Zhang, W.; Wen, J.-L.; Bai, C.-B.; Xing, Y.; Li, Y.-H. Copper/Manganese Cocatalyzed Oxidative Coupling of Vinylarenes with Ketones *Org. Lett.* **2015**, *17*, 4460-4463; (f) Xu, C; Han, Y.; Chen, S.; Xu, D.; Zhang, B.; Shan, Z.; Du, S.; Xu, L.; Gong, P. One-Pot Synthesis of 2-Methyl-1,5-Diaromatic-1H-Pyrroles from Styrene, Acetone and Arylamines using TBHP, Copper(II) Trifluoromethanesulfonate and Sulfamic Acid. *Tetrahedron Lett.* **2018**, *59*, 260-263. See for reviews: (g) Shen, X.; Cao, X.; Zheng, W.; Yang, J.; Shi, Y.; Hu, J.; Wu, X.; Yan, G. Recent Progress in the Research of Acetone in Coupling Reactions. *Chin. J. Org. Chem.* **2017**, *37*, 349-355.

(25) For reviews on the advantages of flow chemistry for photocatalysis, see: (a) Cambié, D.; Bottecchia, C.; Straathof, N. J. W.; Hessel, V.; Noël, T. Applications of Continuous-Flow Photochemistry in Organic Synthesis, Material Science, and Water Treatment. *Chem. Rev.* **2016**, *116*, 10276-10341; (b) Noël, T. A Personal Perspective on the Future of Flow Photochemistry. *J. Flow Chem.* **2017**, *7*, 87-93.

TOC GRAPHIC

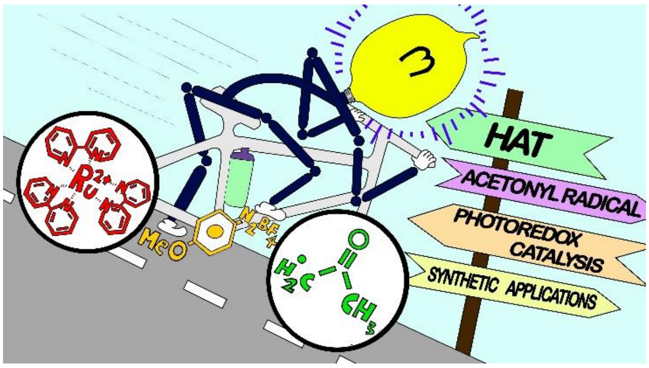
HAT
ACETONYL RADICAL
PHOTOREDOX CATALYSIS
SYNTHETIC APPLICATIONS
Ru 2+
MeO
N2BF4
H2C
O
CH3